Supporting Information

Honey *et al.* 10.1073/pnas.0811168106

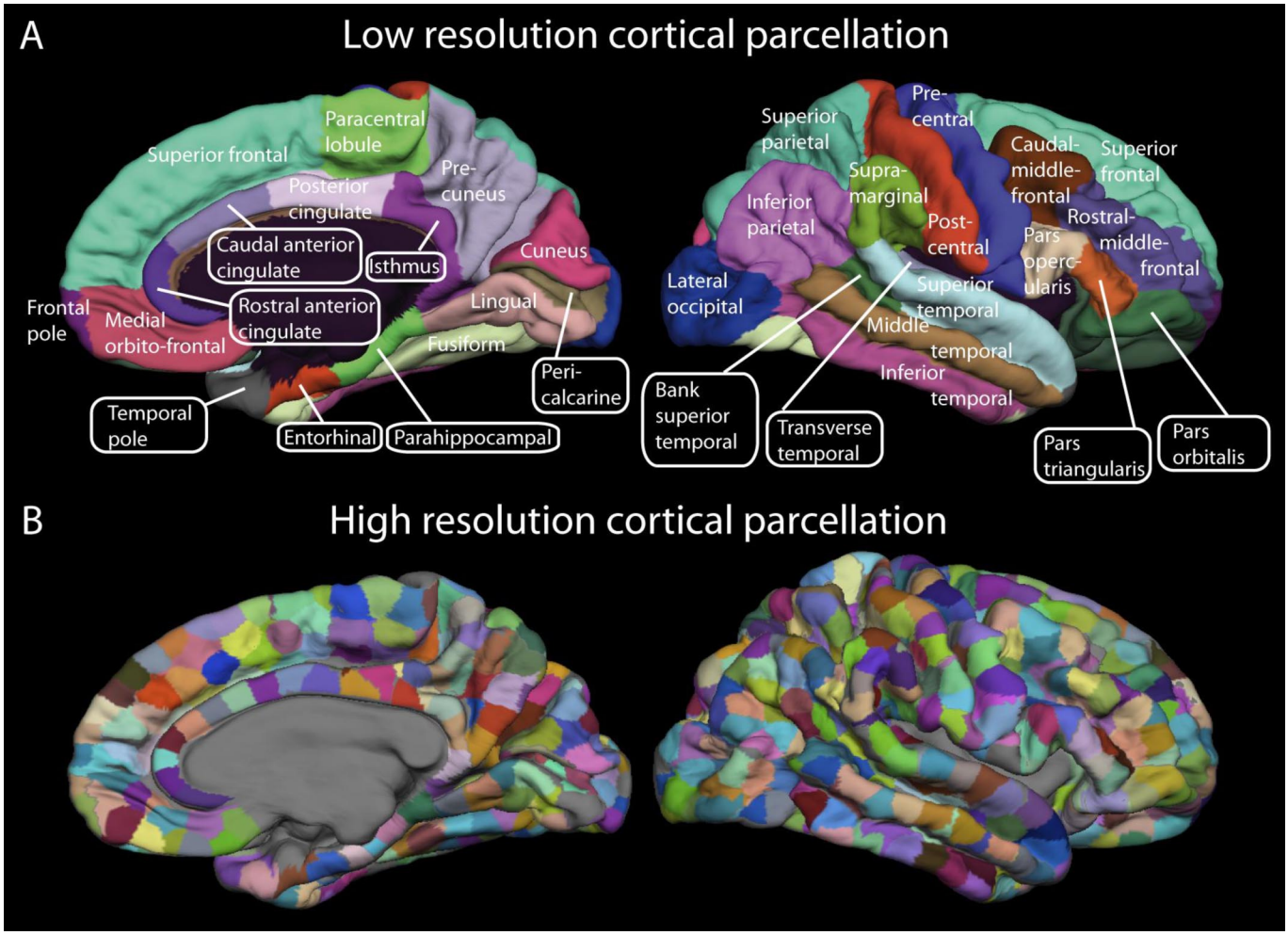

Fig. S1. (*A*) Low-resolution (66-region) and (*B*) high-resolution parcellations (998-ROI) of the cerebral cortex. In the article, the 66 cortical regions are labeled as follows: each label consists of two parts, a prefix for the cortical hemisphere (*r*, right hemisphere, *l*, left hemisphere) and 1 of 33 designators. BSTS, bank of the superior temporal sulcus; CAC, caudal anterior cingulate cortex; CMF, caudal middle frontal cortex; CUN, cuneus; ENT, entorhinal cortex; FP, frontal pole; FUS; fusiform gyrus; IP, inferior parietal cortex; IT, inferior temporal cortex; ISTC, isthmus of the cingulate cortex; LOCC, lateral occipital cortex; LOF, lateral orbitofrontal cortex; LING, lingual gyrus; MOF, medial orbitofrontal cortex; MT, middle temporal cortex; PARC, paracentral lobule; PARH, parahippocampal cortex; POPE, pars opercularis; PORB, pars orbitalis; PTRI, pars triangularis; PCAL, pericalcarine cortex; PSTS, postcentral gyrus; PC, posterior cingulate cortex; PREC, precentral gyrus; PCUN, precuneus; RAC, rostral anterior cingulate cortex; RMF, rostral middle frontal cortex; SF, superior frontal cortex; SP, superior parietal cortex; ST, superior temporal cortex; SMAR, supramarginal gyrus; TP, temporal pole; TT, transverse temporal cortex.

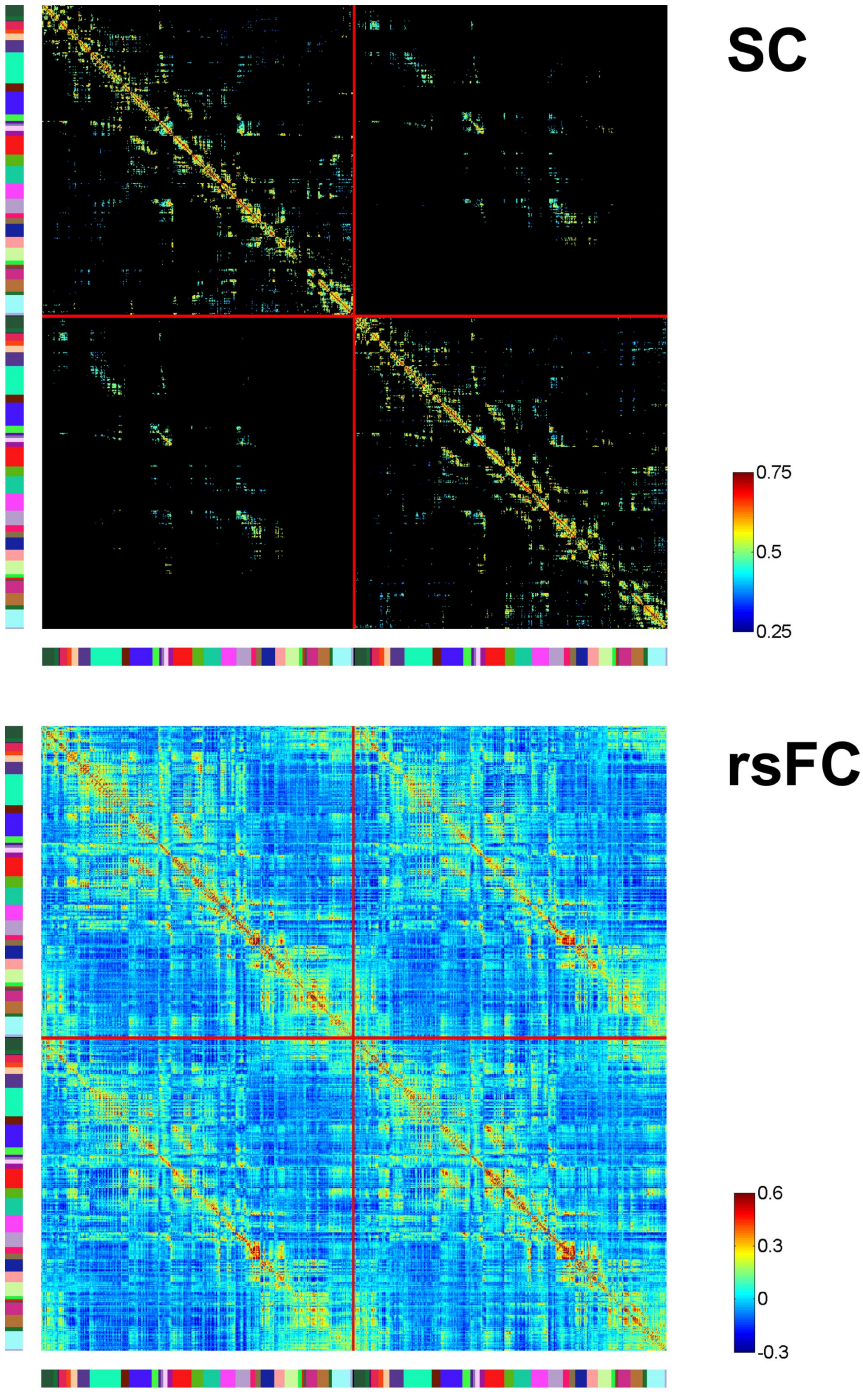

Fig. S2. Matrices of SC and empirical rsFC at the high resolution. Both plots represent averages across all 5 participants, including 2 structural scans for participant A, and 2 repeat functional scans for all 5 participants. The structural connection matrix is averaged after connection strengths were resampled to a Gaussian distribution with a mean of 0.5 and a standard deviation of 0.1. Connections that were present in only 1 out of 5 participants were set to zero strength. The functional connection matrix was computed from BOLD time series obtained for each ROI (see *Methods*). Each correlation value represents an average over 5 participants and 2 repeat scans per participant. The color bars at the left and bottom of the matrices indicate brain regions shown in a corresponding color map in Fig. S1.

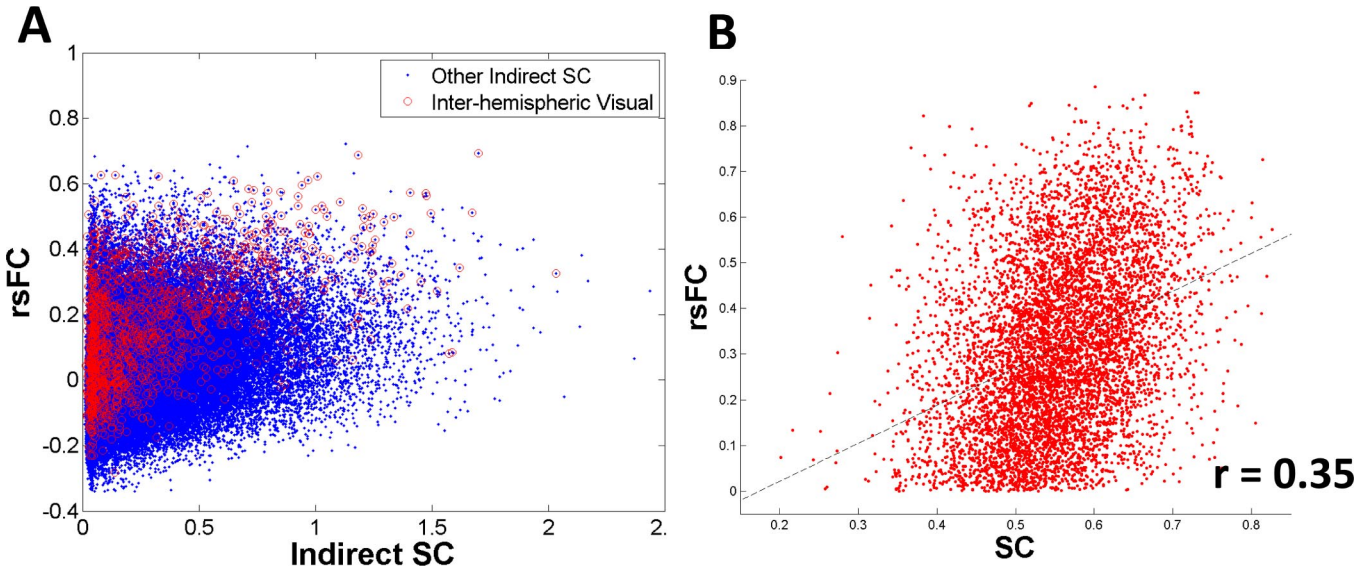

Fig. S3. (*A*) Indirect SC weakly predicts rsFC. The figure shows rsFC plotted against indirect SC (see *Results*) in the average high-resolution data. Plotted are those region pairs linked by at least one of the shortest paths of exactly 2 edges. Highlighted in red are the data points showing indirect SC and rsFC between the visual cortices in left and right hemispheres. Visual cortex ROIs within each hemisphere are those located in pericalcarine cortex, lateral occipital cortex, lingual gyrus, and the cuneus. (*B*) The SC-rsFC relationship for a single session from Participant A, at high resolution (998 ROIs), excluding all ROI pairs that exhibit anticorrelation. The SC-rsFC relationship does not depend on the presence of anticorrelations, nor on regression of a global mean BOLD signal.

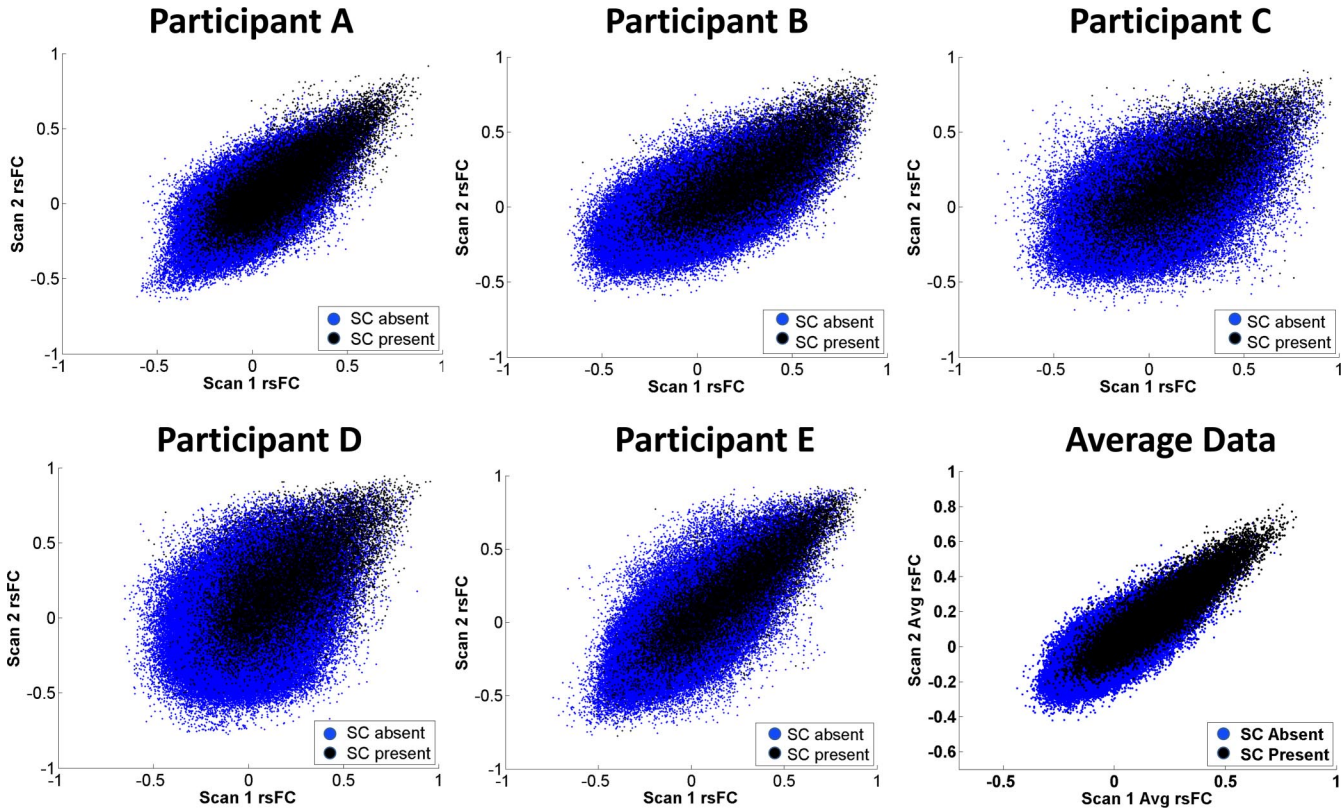

Fig. S4. Increased reliability of rsFC mediated by SC. The scatter plot shows rsFC from Scan 1 against rsFC from Scan 2, using high-resolution data for each of the 5 participants, as well as for participant-averaged SC and rsFC maps. Region-pairs with present SC in black, region-pairs without SC in blue.

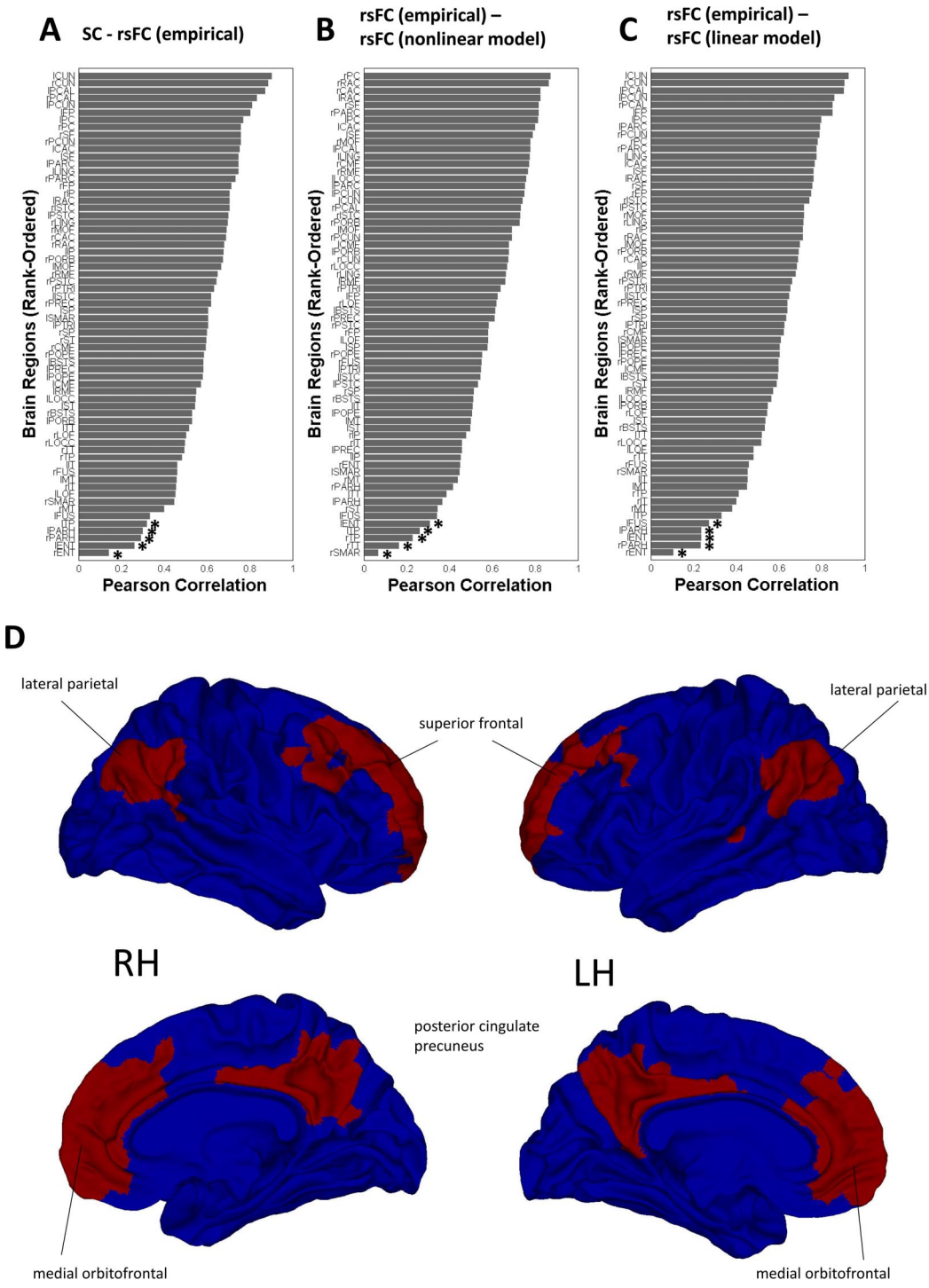

Fig. S5. Rank-ordered distribution of the strength of the relationships between structural connectivity, empirical functional connectivity, and simulated functional connectivity for single brain areas. Data were obtained at the low resolution from SC and rsFC matrices averaged over all 5 participants. (*A*) Pearson correlations for SC versus empirical FC. (*B*) Pearson correlations for empirical FC versus modeled FC (nonlinear model). (*C*) Pearson correlations for empirical FC versus modeled FC (linear model). All correlations except those marked with an asterisk are $P < 0.01$. (*D*) Seed ROIs used for extraction of the DMN shown in Fig. 3. These ROIs were determined as follows. We used published Talairach coordinates for 3 peak foci of task-negative network published by Fox *et al.* (12). These coordinates were (–2, –36, 37) in the posterior cingulate/precuneus [we added a symmetric coordinate at (2, –36, 37)], (–3, 39, –2) and (1, 54, 21) in the medial prefrontal cortex, and (–47, –67, 36) and (53, –67, 36) in the lateral parietal cortex. We identified clusters of 5 ROIs that were closest to each of these 6 target coordinates, resulting in a set of 30 ROIs. These 30 ROIs were used to compute the SC and rsFC maps shown in Fig. 3*C*. Given the empirical rsFC map, we then thresholded this map to obtain a set of 200 ROIs that were most strongly correlated (shown here in dark brown). This set of 200 ROIs covered most of the default-mode network and was used to display the structural connectivity linking these 200 ROIs in Fig. 3*D*.

Table S1. Individual participant SC-rsFC and rsFC-distance correlations and corresponding values from individual runs of the computational model

Participant	Pearson Correlation with rsFC				Model R^2 SC and fiber bivariate
	SC (All)	SC (Present)	Inverse fiber distance	Distance residuals	
66 Regions					
A	0.59	0.74	0.57	0.61	0.59
B	0.56	0.70	0.54	0.59	0.54
C	0.45	0.64	0.50	0.50	0.44
D	0.59	0.71	0.46	0.61	0.50
E	0.60	0.77	0.46	0.70	0.60
Avg participant	0.66	0.82	0.67	0.67	0.69
998 ROIs					
A	0.24	0.42	0.39	0.24	0.20
B	0.24	0.48	0.47	0.23	0.27
C	0.18	0.39	0.40	0.18	0.19
D	0.23	0.42	0.40	0.23	0.20
E	0.22	0.42	0.39	0.24	0.21
Avg participant	0.36	0.53	0.47	0.30	0.30
998 Nodes					
A	0.30	0.34	0.24	0.25	0.12
B	0.39	0.44	0.28	0.35	0.19
C	0.35	0.44	0.31	0.33	0.20
D	0.33	0.37	0.28	0.26	0.15
E	0.35	0.32	0.21	0.25	0.11
Avg participant	0.46	0.52	0.41	0.37	0.28

Individual participant SC-rsFC and rsFC-distance correlations (*Top* 2 sections), and corresponding values from individual runs of the computational model (*Bottom section*). Empirical rsFC is from the first fMRI scan; simulated rsFC is from a single 16 min simulation. The first 2 columns show the SC-rsFC correlations for ″all region pairs″ and for ″region pairs with SC,″ respectively. The third column shows the correlation between rsFC and the inverse of fiber distance, and the fourth column shows the correlation between SC and the residuals of the distance-regression. The fifth column provides the full model R^2 of a bivariate linear regression of rsFC on SC and inverse fiber distance. The bottom row shows the results of each calculation performed using data averaged across participants (it is not the average of the rows above). All correlations are $P << 1e\text{-}3$.

Table S2. Interparticipant SC-rsFC correlations

		Participant rsFC				
All edges		A	B	C	D	E
Participant SC	A	0.237	0.211	0.164	0.205	0.197
	B	0.236	0.240	0.173	0.214	0.218
	C	0.232	0.224	0.180	0.215	0.204
	D	0.234	0.220	0.171	0.231	0.206
	E	0.222	0.212	0.165	0.210	0.225
SC Present edges		A	B	C	D	E
Participant SC	A	0.415	0.407	0.329	0.379	0.383
	B	0.426	0.476	0.353	0.413	0.414
	C	0.450	0.461	0.392	0.422	0.424
	D	0.410	0.429	0.342	0.416	0.380
	E	0.379	0.409	0.345	0.385	0.424

The rsFC map is from the first fMRI scan.

Table S3. Individual participant SC-rsFC and rsFC-distance correlations calculated without resampling of SC values

Participant	Pearson correlation with rsFC				Model R^2 SC and fiber bivariate
	SC (All)	SC (Present)	Inverse fiber distance	Distance residuals	
66 Regions					
A	0.52	0.66	0.55	0.52	0.49
B	0.46	0.57	0.51	0.44	0.41
C	0.38	0.53	0.49	0.38	0.35
D	0.50	0.60	0.45	0.48	0.39
E	0.44	0.57	0.44	0.48	0.38
Avg Participant	0.58	0.71	0.66	0.50	0.57
998 ROIs					
A	0.18	0.34	0.39	0.21	0.19
B	0.15	0.30	0.46	0.13	0.24
C	0.13	0.28	0.40	0.14	0.18
D	0.16	0.30	0.39	0.17	0.18
E	0.16	0.31	0.39	0.19	0.19
Avg Participant	0.30	0.46	0.47	0.27	0.28

rsFC is from the first fMRI scanning session. The SC strength is equal to the number of tractographic streamlines linking two ROIs, divided by the total area of the two ROIs. The first 2 columns show the SC-rsFC correlations for ″all region pairs″ and for ″region pairs with SC,″ respectively. The third column shows the correlation between rsFC and the inverse of fiber distance, and the fourth column shows the correlation between SC and the residuals of the distance-regression. The fifth column provides the full model R^2 of a bivariate linear regression of rsFC on SC and inverse fiber distance. The bottom row shows the results of each calculation performed using data averaged across participants (it is not the average of the rows above).

Table S4. Individual participant SC-rsFC and rsFC-distance correlations, after rsFC maps are Fisher-z transformed and then normalized to zero mean and unit variance across the 998 ROIs of each participant

	Pearson correlation with rsFC				Model R^2 SC and fiber bivariate
Participant	SC (All)	SC (Present)	Inverse fiber distance	Distance residuals	
66 Regions					
A	0.60	0.75	0.55	0.64	0.58
B	0.58	0.71	0.52	0.61	0.54
C	0.45	0.64	0.49	0.52	0.44
D	0.61	0.71	0.45	0.62	0.51
E	0.62	0.77	0.44	0.72	0.61
Avg Participant	0.68	0.82	0.66	0.68	0.69
998 ROIs					
A	0.25	0.41	0.38	0.24	0.20
B	0.25	0.47	0.46	0.24	0.25
C	0.19	0.39	0.39	0.19	0.18
D	0.24	0.41	0.38	0.24	0.20
E	0.24	0.42	0.38	0.26	0.21
Avg Participant	0.38	0.53	0.46	0.32	0.30

The first 2 columns show the SC-rsFC correlations for ″all region pairs″ and for ″region pairs with SC,″ respectively. The third column shows the correlation between rsFC and the inverse of fiber distance, and the fourth column shows the correlation between SC and the residuals of the distance-regression. The fifth column provides the full model R^2 of a bivariate linear regression of rsFC on SC and inverse fiber distance. The bottom row shows the results of each calculation performed using data averaged across participants (it is not the average of the rows above).

Other Supporting Information Files

SI Appendix